Mem. Fac. Sci. Eng. Shimane Univ.
Series A
30, pp. 75-84 (1997)

Cascaded Realization of Complex Adaptive IIR Notch Filters

Shotaro NISHIMURA[1] and Hai-Yun JIANG[2]

[1]*Department of Electronic and Control Systems Engineering, Shimane University, Matsue, Japan.*
[2]*Graduate School of Science, Shimane University, Matsue, Japan.*
(Received December 31, 1996)

Abstract

In this paper, we present a new structure for complex adaptive IIR notch filter which is useful for the detection of complex sinusoids in communication and radar systems. The proposed structure is based on the direct form first-order complex notch filter using gradient-based algorithm. A quantitative analysis for convergence properties is developed. It has been shown that the convergence speed does not depend on the variance of input white noise. The effects of colored Gaussian noise to convergence speed have been analyzed. By using the proposed first-order section, a new cascaded structure for complex adaptive notch filter has been shown. The results of computer simulation are shown which confirm the theoretical prediction.

1 Introduction

Adaptive digital notch filter has found many applications such as the detection of sinusoids in noise or cancelling a periodic interference from signal measurements[1-4]. The enhancement of complex sinusoids is also widely used in communication and radar systems, where the signal consists of in-phase and quadrature-phase components[5,6].

In this paper, we present a class of new complex coefficient adaptive notch filter using gradient-based adaptive algorithm, which does not require any division. A quantitative analysis for convergence behavior of proposed structure has been presented. Also, the cascade realization based on proposed first-order section is presented.

The organization of the paper is as follows. The structures of first-order complex adaptive notch filter are presented in Sect. 2. In Sect. 3, we present a method of obtaining the necessary iteration of convergence. Section 4 introduces a new structure of cascaded complex coefficient adaptive notch filter. Results of computer simulation that confirm the developed theories are presented in Sect. 5. Finally, Sect. 6 contains the concluding remarks.

2 Filter Structure

Figure 1 shows a block diagram of first-order complex coefficient adaptive notch filter considered here. The input data are written as

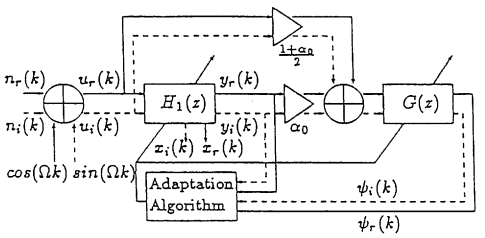

Fig. 1. Block diagram of first-order complex adaptive notch filter.

$$u(k)=Ae^{j(\Omega k+\theta)}+n(k),\ k=0,\ 1,\ 2,\ \cdots, \tag{1}$$

where k is the time index, Ω is an unknown angular frequency of the input sinusoid. $n(k)$ is a sequence of complex Gaussian random variables given by $n(k)=n_r(k)+jn_i(k)$, where $n_r(k)$ and $n_i(k)$ are real processes with zero mean and variance σ_n^2.

The transfer function from input to notch filter output is given by

$$H(z)=\frac{1+\alpha_0}{2}\frac{1-e^{j\omega_1(k)}z^{-1}}{1-\alpha_0 e^{j\omega_1(k)}z^{-1}}, \tag{2}$$

where ω_1(k) is a variable coefficient of $H(z)$[5,6]. The notch angular frequency of the filter is obtained by $\omega_1(k)$.

In this paper, we use the simple gradient algorithm which does not require any matrix inversion. For the adaptive notch filter, $\omega_1(k)$ is chosen to minimize the notch filter output power, $y(k)$y*(k), where "*" denotes a complex conjugate.

The adaptation algorithm considered in this paper is given by

$$\omega_1(k+1)=\omega_1(k)-\mu Re[y(k)\psi^*(k)], \tag{3}$$

where μ is a step size controlling the convergence rate. $\psi(k)$ is the differential of $y(k)$ with respect to $\omega_1(k)$, and is referred to as the gradient signal. $\psi(k)$ is generated by the circuit whose transfer function is given by

$$G(z)=\frac{je^{j\omega_1(k)}z^{-1}}{1-\alpha_0 e^{j\omega_1(k)}z^{-1}}. \tag{4}$$

The input to this circuit is given by $u_1(k)=\alpha_0 y(k)-(1/2)(1+\alpha_0)u(k)$. This filter will be referred to as a Type I filter.

In Figure 1, the transfer function from input $u(k)$ to $x_1(k)$ is given by (4) multiplied by $(1+\alpha_0)/2$. By using $y(k)$ and $x_1(k)$, we can obtain the simplified adaptation algorithm,

$$\omega_1(k+1)=\omega_1(k)+\mu Re[y(k)x_1^*(k)]. \tag{5}$$

This filter will be referred to as a Type II filter. The signal $x_1(k)$ is called the simplified gradient signal.

3 Convergence Analysis

Referring the magnitude and phase responses of transfer functions $H(z)$ and $G(z)$, the convergence characteristics of proposed coefficient update algorithm have been analyzed. If the input signal is given by the sum of a sinusoid and additive Gaussian noise, $y(k)$ and $\psi(k)$ can be expressed as

$$y(k)=s_1(k)+n_1(k),\ \psi(k)=s_2(k)+n_2(k), \tag{6}$$

$$s_1(k)=AA_Ne^{j(\Omega k+\theta_N)}, \tag{7}$$

$$s_2(k)=AA_BA_Ge^{j(\Omega k+\theta_B+\theta_G)}, \tag{8}$$

where A_N and A_G are magnitude responses of transfer functions, $H(z)$ and $G(z)$, respectively, and θ_N and θ_G are phase responses of those transfer functions. A_B and θ_B are the magnitude and phase responses of transfer function from $u(k)$ to $u_1(k)$, respectively. $n_1(k)$ and $n_2(k)$ are noise terms containing in $y(k)$ and $\psi(k)$.

From (3), (6), (7) and (8), an average step size for one iteration of coefficient update at time k can be given by

$$\begin{aligned}E[\delta\omega_1(k)]&=E[\omega_1(k+1)-\omega_1(k)]\\&=-\mu A^2A_NA_BA_Gcos(\theta_N-\theta_B-\theta_G)\\&\quad-\mu Re[E(n_1(k)n_2^*(k))].\end{aligned} \tag{9}$$

where $E[\bullet]$ denotes the expectation operator. The second term of the right-hand side of (9) can be obtained from the following complex integration along the unit circle in the z-plane.

$$Re[E(n_1(k)n_2^*(k))]=2Re[\frac{\sigma_n^2}{2\pi j}\oint \phi(z)H^*(z)H_B(z^{-1})z^{-1}dz], \tag{10}$$

where

$$H_B(z)=(\alpha_0H(z)-\frac{1+\alpha_0}{2})\,G(z). \tag{11}$$

In (10), $\phi(z)$ is a z-transform of the auto-correlation function of input noise $n(k)$.

If the input noise $n_r(k)$ and $n_i(k)$ are assumed to be sequences of independent zero mean white Gaussian random variable, it follows $Re[E(n_1(k)n_2^*(k))]=0$. Figure 2 plots the values of $-A^2A_NA_BA_Gcos(\theta_N-\theta_B-\theta_G)$ in (9) for $A=1$ and Ω as a parameter. When $\omega_1(k)=\Omega$, it follows $E[\delta\omega_1(k)]=0$. If $\omega_1(k)<\Omega$, the values of $E[\delta\omega_1(k)]$ is positive and if $\omega_1(k)>\Omega$, it is negative. From the above analysis it should be noted that the convergence speed of adaptive complex notch filter does not depend on variance of input white noise. The convergence curves can be calculated from (9) by using step-by-step method given by

$$\omega_1(k+1)=\omega_1(k)+E[\delta\omega_1(k)]. \tag{12}$$

It should be noted that the similar results can be obtained for the case of Type II filter.

Next, we consider the effect of input colored Gaussian noise to the convergence characteristics

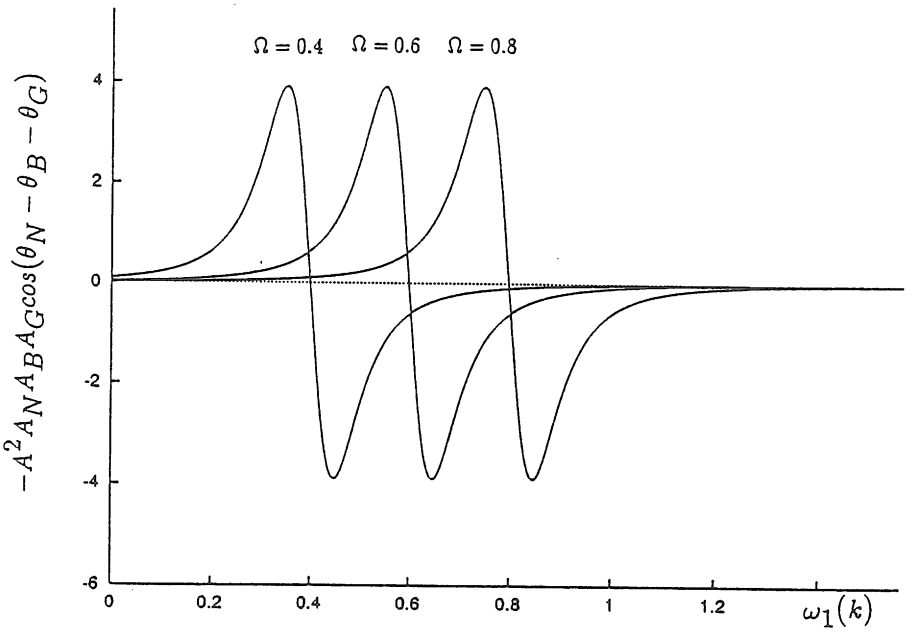

Fig. 2. Numerical results obtained from (9).

of variable coefficient. For simplicity it is assumed that the real and imaginary part of input noise, $n_r(k)$ and $n_i(k)$, are generated by same first-order autoregressive process with a transfer function

$$F(z)=\frac{\sqrt{1-b^2}}{1-bz^{-1}}\ ,-1<b<1, \tag{13}$$

where the input to this circuit is the white Gaussian noise with mean zero and variance σ_n^2. In this case $\phi(z)$ becomes

$$\phi(z)=F(z)F(z^{-1})\sigma_n^2. \tag{14}$$

From (2), (11), and (14), we get the analytical expression for complex integration in the right-hand side of (10) and it has been shown in Table 1.

Figure 3 plots the values of $-Re[E(n_1(k)n_2^*(k))]$ obtained from Table 1 with b in (13) as a parameter. From Fig. 2 and Fig. 3, it can be observed that if $0<b<1$, the second term of the right-hand side of (9) is negative. Then it follows for $\omega_1(k)>\Omega$, the addition of the second term has the effect of increasing the absolute value of $E[\delta\omega_1(k)]$. On the other hand, if $\omega_1(k)<\Omega$, the absolute value of $E[\delta\omega_1(k)]$ decreases due to the addition of above noise term in (9).

From above observation we can infer that if b is positive and $F(z)$ of (13) has low-pass characteristics, the variable coefficient $\omega_1(k)$ converges faster when initial value of $\omega_1(k)$, $\omega_1(0)$, is larger than Ω. While $\omega_1(k)$ converges slower due to the input colored noise when $\omega_1(0)<\Omega$.

Table 1 $Re[E(n_1(k)n_2^*(k))]$ for colored noise

$$Re[E(n_1k)n_2^*(k))]=2Re[\frac{\sigma_n^2}{2\pi j}\oint \phi(z)H^*(z)H_B(z^{-1})z^{-1}dz]$$

$$=2\sigma_n^2(K_1\frac{C_1C_2+C_3C_4}{C_1^2C_3^2}+K_2\frac{D_1D_2+D_3D_4}{D_1^2D_3^2})$$

where

$$K_1=\frac{(1+\alpha_0)(1-\alpha_0^2)b}{4}$$

$$K_2=\frac{\alpha_0(b^2-1)}{4}$$

$$C_1=b(1+2\alpha_0^2)+\alpha_0^2b^3\cos2\omega_1-\alpha_0(2b^2+1+\alpha_0^2b^2)\cos\omega_1$$

$$C_2=b\sin\omega_1$$

$$C_3=-b^3\alpha_0^2\sin 2\omega_1+\alpha_0(2b^2-1+\alpha_0^2b^2)\sin\omega_1$$

$$C_4=b\cos\omega_1-1$$

$$D_1=\alpha_0(1+b^2)\cos\omega_1-b-\alpha^2b\cos2\omega_1$$

$$D_2=-\sin\omega_1$$

$$D_3=-\alpha_0^2b\sin2\omega_1+\alpha_0(1+b^2)\sin\omega_1$$

$$D_4=\cos\omega_1$$

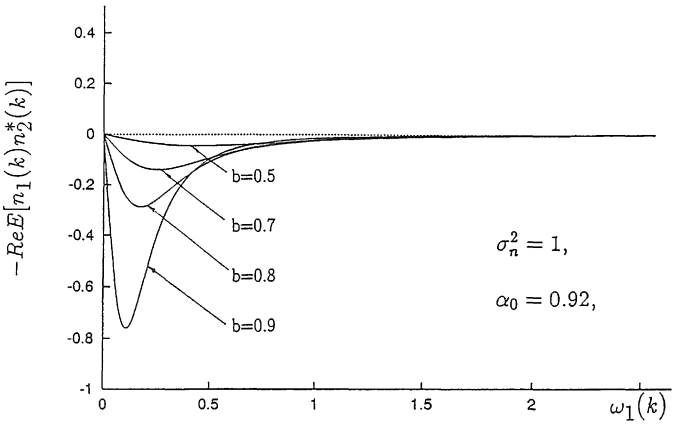

Fig. 3. Numerical results obtained from Table 1.

4 Cascade Structure

In this section, a new complex adaptive notch filter for detecting multiple sinusoids will be

described. The proposed structure is based on a cascade of Type II filter given in Sect. 2. Fig. 4 shows the proposed complex adaptive notch filter structure for tracking N sinusoids. The transfer function of N *th* order notch filter is given by

$$Y(z)=\prod_{i=1}^{N}\frac{1+\alpha_0}{2}\frac{1-e^{j\omega_i(k)}z^{-1}}{1-\alpha_0 e^{j\omega_i(k)}z^{-1}} \tag{15}$$

The variable coefficient of each section is chosen to minimize the output power $y_N(k)y_N^*(k)$, where $y_N(k)$ is the output of the N *th* order notch filter with transfer function $Y(z)$. The updating formula of the proposed structure becomes

$$\omega_i(k+1)=\omega_i(k)+\mu y_N(k)\psi_i(k) \quad i=1, 2, \cdots N.$$

The gradient signal for the i *th* coefficient, $\psi_i(k)$, is generated by using the *N-i th* order notch filter with transfer function

$$X(z)=\prod_{l=i+1}^{N}\frac{1+\alpha_0}{2}\frac{1-e^{j\omega_l(k)}z^{-1}}{1-\alpha_0 e^{j\omega_l(k)}z^{-1}} \tag{16}$$

for

$$i=1, 2, \cdots, N-1, \tag{17}$$

and

$$X(z)=1, \textit{for } i=N, \tag{18}$$

where an input to this notch filter is given by the simplified gradient signal of *i th* section, $x_i(k)$.

5 Simulation Results

Some numerical examples will be presented in order to demonstrate the results in Sect. 3 and Sect. 4.

In the first experiment, the input sinusoid has unit magnitude and is corrupted by the colored Gaussian noise with $\sigma_n^2=2.0$. The angular frequency of the input sinusoid, Ω, was $\frac{\pi}{6}$. Figure 5 shows the convergence characteristics of $\omega_1(k)$. Here, the learning curves are estimated by taking an average of 100 individual runs of $\omega_1(k)$ versus k. Each run had a different random sequence.

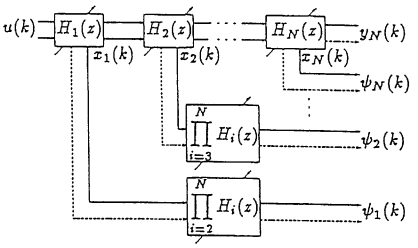

Fig. 4. A cascaded realization.

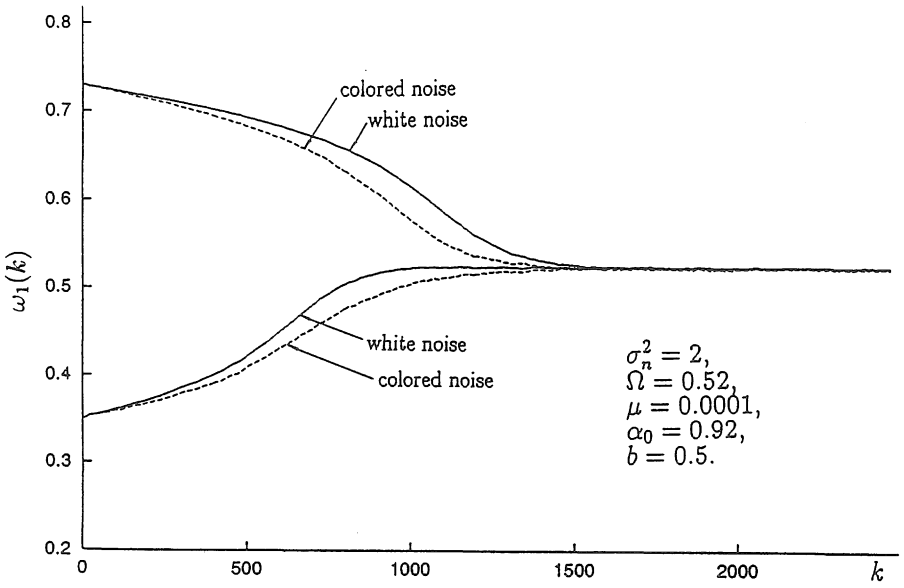

Fig. 5. Simuleted results for the convergence behavior of $\omega_1(k)$.

The simulated values of $\omega_1(k)$ for colored noise are shown, along with the curves for white input noise. For colored noise, the values of b in (13) is fixed at 0.5. The values of μ and α_0 are fixed at 0.0001 and 0.92, respectively. Initial value, $\omega_1(0)$ was chosen to be 0.73 or 0.35. It should be noted that when the value of $\omega_1(0)$ is chosen to be 0.73, the convergence speed for colored input noise becomes faster than for white input noise as expected from the theory in Sect. 3. It is also found that when $\omega_1(0)$ is equal to 0.35, the convergence speed for colored input noise becomes slower than that for white input noise. The convergence curves predicted by using (12) have been shown in Fig. 6. It should be noted that the simulated and theoretical results show very close match.

In the second experiment we demonstrate the performance of the proposed cascaded realization for $N=2$. The input is given by $e^{j0.7k}+e^{j0.5k}+\sqrt{0.5}(n_r(k)+jn_i(k))$, where $n_r(k)$ and $n_i(k)$ are independent colored noise processes with $\sigma_n^2=2.0$. The same values of μ, α_0 and b are used as in the Figs. 5 and 6. Figure 7 shows the convergence behavior of coefficients, when the initial values of $\omega_1(k)$ and $\omega_2(k)$ are chosen to be 0.65. It is found that $\omega_i(k)$, $i=1, 2$, converge to the optimal values of 0.7 and 0.5.

With the third experiment, we tested the convergence characteristics for the input given by $e^{j0.7k}+0.3e^{j0.5k}+\sqrt{0.5}(n_r(k)+jn_i(k))$. Learning curves of $\omega_i(k)$ for initial values, $\omega_i(0)=0.65$, $i=1, 2$, are shown in Fig. 8, using the same parameters as in the previous example. In this case, $\omega_1(k)$ converges to the optimal value of 0.7, while $\omega_2(k)$ converges to 0.0, due to the input colored noise.

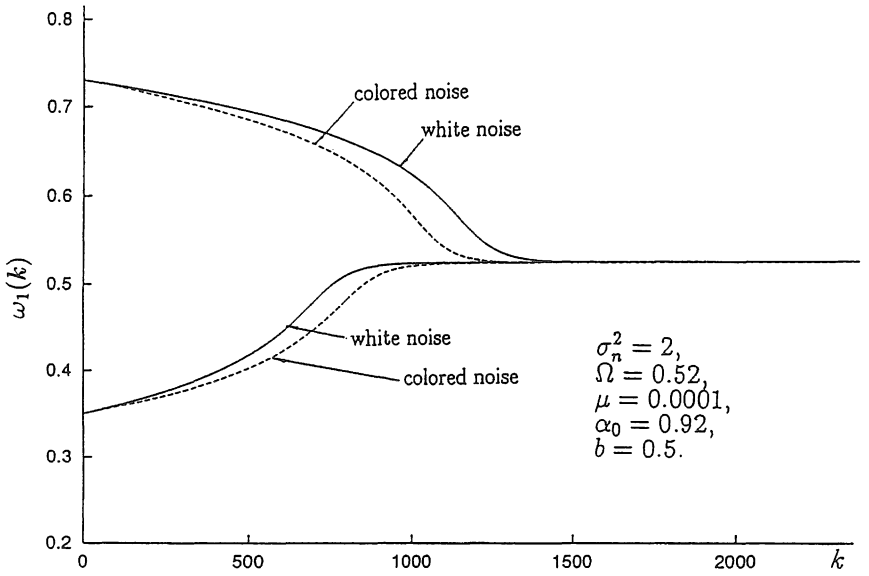

Fig. 6. Theoretical results for the convergence behavior of $\omega_1(k)$.

Fig. 7. The convergence behavior of $\omega_i(k)$, $i=1, 2$, for $u(k)=e^{j0.7k}+e^{j0.5k}+\sqrt{0.5}(n_r(k)+jn_i(k))$

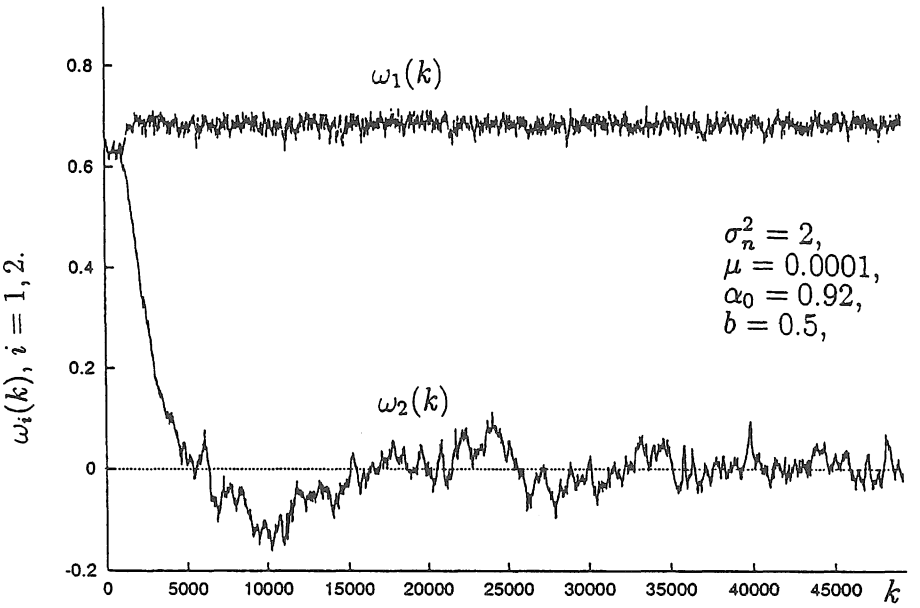

Fig. 8. The convergence behavior of $\omega_i(k)$, $i=1, 2$, for $u(k)=e^{j0.7k}+0.3e^{j0.5k}+\sqrt{0.5}(n_r(k)+jn_i(k))$

6 Conclusions

In this paper, a class of new structure for complex adaptive notch filter has been presented. A quantitative analysis of convergence properties was developed for the first-order section using gradient algorithm. The effects of colored input noise generated by first-order autoregressive model have been investigated. By using the first-order section, a new cascaded structure has been developed, which is suitable for detecting and enhancing multiple sinusoids. The proposed algorithms have the advantage that a stability check is not required.

A quantitative analysis of convergence properties is currently being investigated for the proposed cascaded structure.

Reference

1) K. Martin and M. T. Sun, "Adaptive filter suitable for realtime spectral analysis," IEEE Trans. Circuits Syst., vol. CAS-33, pp. 2118-2129, Feb. 1986.

2) S. Nishimura, J. K. Kim and K. Hirano, "Mean-squared error analysis of an adaptive notch filter," in Proc. IEEE Int. Symp. Circuits Syst., May 1989, pp.732-735.

3) S. Nishimura, J. K. Kim and K. Hirano, "Steady-state analysis of adaptive notch filter for detection of multiple sinusoids," in Proc. IEEE Int. Symp. Circuits Syst., May 1990, pp. 3162-3164.

4) J. F. Chicharo and T. S. Ng, "Gradient-based adaptive IIR notch filtering for frequency estimation," IEEE

Trans. Acoust., Speech, Signal Processing, vol. 38, pp. 769-777, May 1990.
5) S. C. Pei and C. C. Tseng, " Complex adaptive IIR notch filter algorithm and its applications," IEEE Trans. Circuits Syst. II, vol. 41, pp. 158-163, Feb. 1994.
6) C. C. Ko and C. P. Li, "An adaptive IIR structure for the separation, enhencement, and tracking of multiple sinusoids," IEEE Trans. Signal Processing, vol. 42, pp. 2832-2834, Oct. 1994.